Journal of Hazardous Materials 183 (2010) 233–241

Contents lists available at ScienceDirect

Journal of Hazardous Materials

journal homepage: www.elsevier.com/locate/jhazmat

Adsorption and desorption of Cu(II), Cd(II) and Pb(II) ions using chitosan crosslinked with epichlorohydrin-triphosphate as the adsorbent

Rogério Laus, Thiago G. Costa, Bruno Szpoganicz, Valfredo T. Fávere*

Departamento de Química, Universidade Federal de Santa Catarina, 88040-900, Florianópolis, SC, Brazil

ARTICLE INFO

Article history:
Received 16 November 2009
Received in revised form 5 July 2010
Accepted 6 July 2010
Available online 13 July 2010

Keywords:
Chitosan
Epichlorohydrin
Triphosphate
Adsorption
Desorption

ABSTRACT

In this study, chitosan (CTS) was crosslinked with both epichlorohydrin (ECH) and triphosphate (TPP), by covalent and ionic crosslinking, respectively. The resulting new CTS–ECH–TPP adsorbent was characterized by CHN analysis, EDS, FTIR spectroscopy, TGA and DSC, and the adsorption and desorption of Cu(II), Cd(II) and Pb(II) ions in aqueous solution were investigated. Potentiometric studies were also performed and revealed three titratable protons for each pK_a value of 5.14, 6.76 and 9.08. The results obtained showed that the optimum pH values for adsorption were 6.0 for Cu(II), 7.0 for Cd(II) and 5.0 for Pb(II). The kinetics study demonstrated that the adsorption process proceeded according to the pseudo-second-order model. Three isotherm models (Langmuir, Freundlich and Dubinin-Radushkevich) were employed in the analysis of the adsorption equilibrium data. The Langmuir model resulted in the best fit and the new adsorbent had maximum adsorption capacities for Cu(II), Cd(II) and Pb(II) ions of 130.72, 83.75 and 166.94 mg g^{-1}, respectively. Desorption studies revealed that HNO_3 and HCl were the best eluents for desorption of Cu(II), Cd(II) and Pb(II) ions from the crosslinked chitosan.

1. Introduction

The increasing levels of toxic heavy metal ions discharged to the environment have received considerable attention due to the adverse effects on receiving waters. The potential sources of heavy metal ions in wastewaters include fertilizers, fungicides, metals used in manufacturing, paints, pigments, and batteries. These ions are a hazard to public health and the environment when discharged inappropriately. Many methods such as ion exchange, precipitation, adsorption, and membrane processes have been used for the removal of toxic metal ions. In particular, adsorption is recognized as an effective and economic method for the removal of pollutants from wastewaters. However, because this process is expensive, low-cost biosorbents have been given increasing attention as they can significantly reduce the cost of an adsorption system [1,2,3].

In particular, chitosan (CTS) has been studied due to its high capacity to adsorb heavy metal ions, dyes, and proteins. Other useful features of CTS include its abundance, non-toxicity, hydrophilicity, biocompatibility, biodegradability, and antibacterial and antimicrobial properties [4,5,6,7,8]. It has several potential applications, for instance, in biomedical products, cosmetics, pharmaceutical processes, food processing, agricultural chemicals, wastewater treatment, and metal chelating agents [9,10,11].

Chitosan is obtained from the deacetylation of the natural biopolymer chitin, found in crustaceous shells, insects, and fungal cell walls. CTS consists of β-(1,4)-2-acetamido-2-deoxy-β-D-glucose and β-(1,4)-2-amino-2-deoxy-β-D-glucose units and contains high contents of amino and hydroxyl groups, which favors the modification of this biopolymer and the introduction of new functional groups [6,12,13].

CTS is soluble in most dilute mineral acids, except in sulfuric acid solutions and dilute organic acids, such as acetic, propionic, formic and lactic acids. Consequently, its chemical stability needs to be reinforced through treatments using crosslinking agents for application in acidic media. This treatment induces new linkages between the chitosan chains allowing the polymer to be highly resistant to dissolution, even in harsh solutions, such as hydrochloric acid [14,15]. The crosslinking procedure may be performed by reaction of CTS with different agents such as glutaraldehyde (GLA), ethylene glycol diglycidyl ether (EGDE) and epichlorohydrin (ECH). Triphosphate (TPP) has also been proposed as a possible crosslinking agent [3,4,16].

ECH is a crosslinking mono-functional agent used to form covalent bonds with the carbon atoms of the hydroxyl groups of chitosan, resulting in the rupturing of the epoxide ring and the removal of a chlorine atom [17].

TPP is a non-toxic multivalent anion that can form cross-links by ionic interaction between the positively charged amino groups of chitosan and the negatively charged counterion of the TPP molecules. This interaction can be controlled by the charge density

* Corresponding author. Tel.: +55 48 3721 6844; fax: +55 48 3721 6850.
E-mail address: favere@qmc.ufsc.br (V.T. Fávere).

0304-3894/$ – see front matter © 2010 Elsevier B.V. All rights reserved.
doi:10.1016/j.jhazmat.2010.07.016

of TPP and chitosan, which is dependent on the pH of the solution [4,5,18,19].

Pentasodium TPP can be dissolved in water to dissociate into OH^- and triphosphoric ions, as shown in the following dissociation reactions [5,20].

$$Na_5P_3O_{10} + 5H_2O \rightarrow 5Na^+ + H_5P_3O_{10} + 5OH^- \quad (1)$$

$$H_5P_3O_{10} + OH^- \rightleftharpoons H_4P_3O_{10}{}^- + H_2O \quad (pK_{a1} = -\infty) \quad (2)$$

$$H_4P_3O_{10}{}^- + OH^- \rightleftharpoons H_3P_3O_{10}{}^{2-} + H_2O \quad (pK_{a2} = 1.1) \quad (3)$$

$$H_3P_3O_{10}{}^{2-} + OH^- \rightleftharpoons H_2P_3O_{10}{}^{3-} + H_2O \quad (pK_{a3} = 2.3) \quad (4)$$

$$H_2P_3O_{10}{}^{3-} + OH^- \rightleftharpoons HP_3O_{10}{}^{4-} + H_2O \quad (pK_{a4} = 6.3) \quad (5)$$

$$HP_3O_{10}{}^{4-} + OH^- \rightleftharpoons P_3O_{10}{}^{5-} + H_2O \quad (pK_{a5} = 8.9) \quad (6)$$

In this study, we prepared a novel type of modified chitosan by incorporating epichlorohydrin (via a covalent crosslinking reaction) and triphosphate (via an ionic crosslinking reaction), and evaluated its potential in terms of the adsorption and desorption of Cu(II), Cd(II) and Pb(II) ions.

2. Experimental

2.1. Instrumentation

The chitosan–epichlorohydrin–triphosphate (CTS–ECH–TPP) adsorbent was prepared using a Dispersor Extratur® Quimis Q252 M. The CHN elemental analysis was performed with a Carlo Erba CHNS-O-E1110 analyzer. Scanning electron microscopy (SEM) and energy dispersive X-ray spectroscopy (EDS) were performed using a JEOL JSM-6390LV instrument. Infrared (IR) spectra were obtained with KBr pellets in the range of 2000–450 cm^{-1}, using a PerkinElmer 2000 FT-IR spectrometer. Thermogravimetric analysis (TGA) and differential scanning calorimetry (DSC) were carried out using a Shimadzu TGA 50 and a Shimadzu DSC 50, respectively. Both analytical techniques were carried out with a heating rate of 10 °C min^{-1}, under nitrogen flow at a rate of 50 mL min^{-1}. DSC curves were obtained from the first heating runs. The potentiometric studies were carried out with an automatic Metrohm Titrino Plus 848 titrator, coupled to a combined glass electrode (Ag/AgCl). The pH of the solutions was adjusted using a Corning pH/ion analyzer 350. A Marconi MA 832 mini-shaker thermostatic bath was used in the adsorption and desorption experiments. The concentration of Cu(II), Cd(II) and Pb(II) ions was determined by flame atomic absorption spectroscopy (FAAS) using a Varian SpectrAA 50 spectrometer equipped with an air-acetylene flame atomizer and a Hitachi hollow cathode lamp specific for each metal ion. The lamp was operated under the conditions recommended by the manufacture. Also, conventional values for the wavelength, slit width and burner height were applied. The aspiration rate was 6 mL min^{-1}.

2.2. Materials and reagents

Chitosan was purchased from Purifarma Company (Brazil) with a degree of deacetylation of 90% and molecular weight of 122.74 kg mol^{-1}. Epichlorohydrin was obtained from Synth (Brazil). Pentasodium triphosphate was purchased from Fluka (Switzerland). The working standard solutions of Cu(II), Cd(II) and Pb(II) were prepared using appropriate dilutions of stock solutions (1000 mg L^{-1}), which were obtained from dilutions of Fluka® (Sigma–Aldrich, Germany) ampoules ($CuCl_2$, $CdCl_2$ and $Pb(NO_3)_2$ in water, respectively). The following buffer solutions were used at a concentration of 0.1 mol L^{-1} to adjust the pH: chloroacetic/sodium chloroacetate (pH 2 and 3), acetic acid/sodium acetate (pH 4–6), Tris(hydroxymethyl)aminomethane adjusted with diluted HCl solution (pH 7–9) and ammonium hydroxide/ammonium chloride (pH 10 and 11). All solutions were prepared with distilled water. All reagents were of analytic grade and used without further purification.

2.3. Preparation of crosslinked chitosan

The CTS–ECH–TPP adsorbent was prepared by the phase inversion method. For the preparation of the crosslinked chitosan, powdered chitosan was dissolved in 1% (v/v) acetic acid solution to produce a viscous solution with 1% (w/v) chitosan. An aliquot of 10 mL of 12.5 mol L^{-1} ECH was added to the chitosan solution and maintained at 60 °C for 2 h. The chitosan/ECH molar ratio used in this study was 1.0/0.5, as optimized by Chen et al. [1]. Subsequently, 50 mL of 0.1 mol L^{-1} NaOH was added and the system was boiled for 3 h. Finally, 100 mL of 5% (w/v) TPP solution was added dropwise to the epichlorohydrin crosslinked chitosan solution under constant stirring at 6000 rpm for 10 min. The CTS–ECH–TPP sample was initially filtered and washed with distilled water to remove the excess of crosslinking agents and then dried in a vacuum. The CTS–ECH–TPP particle size was 100–150 μm, obtained using appropriate sieves, and did not show a well-defined shape in the SEM analysis. Fig. 1 shows the structure of the new adsorbent formed by crosslinking chitosan with ECH (covalent crosslinking) and with TPP (ionic crosslinking).

2.4. Potentiometric measurements

The potentiometric studies were performed in a cell cooled mechanically in a thermostatic bath maintained at 25.00 ± 0.05 °C. A mass of 100 mg CTS–ECH–TPP was weighed directly into this cell and 50 mL of water was added along with 1.5 mL of 0.1 mol L^{-1} HCl solution for protonation of phosphate groups and to obtain a good dispersion of the adsorbent. The system was kept under argon flow to eliminate the presence of atmospheric CO_2. For the titrations a standard CO_2-free KOH solution (0.104 mol L^{-1}) was used, to which aliquots of 0.050 mL were added until pH 12, using an automatic titrator coupled to a combined glass electrode, which was calibrated directly in the cell with diluted HCl solution before starting the titrations. The protonation/deprotonation constants were calculated using the BEST7 program and species distribution curves of the adsorbent were obtained with the SPECIES program [21].

2.5. Adsorption and desorption experiments

All experiments to investigate the adsorption (effect of pH, kinetics and isotherms) and desorption of Cu(II), Cd(II) and Pb(II) ions onto the CTS–ECH–TPP adsorbent were carried out in batch tests, using a thermostated bath at 25 °C, under constant stirring of 200 rpm.

The amount of metal ion adsorbed was calculated according to the following equation:

$$q = \frac{(C_o - C_e)V}{m} \quad (7)$$

where q is the amount (mg g^{-1}) of metal ions adsorbed by the CTS–ECH–TPP, C_o and C_e are the metal concentrations (mg L^{-1}) in the solution initially and after adsorption, respectively, V is the volume (L) of the solution and m is the mass (g) of adsorbent used.

2.5.1. Effect of pH

Samples (50.0 mg) of the CTS–ECH–TPP adsorbent were placed in a series of flasks containing 50.0 mL of a solution of each metal ion at an initial concentration of 50 mg L^{-1}, buffered within a pH range of 2–11. After 24 h, the final pH value was measured and aliquots of

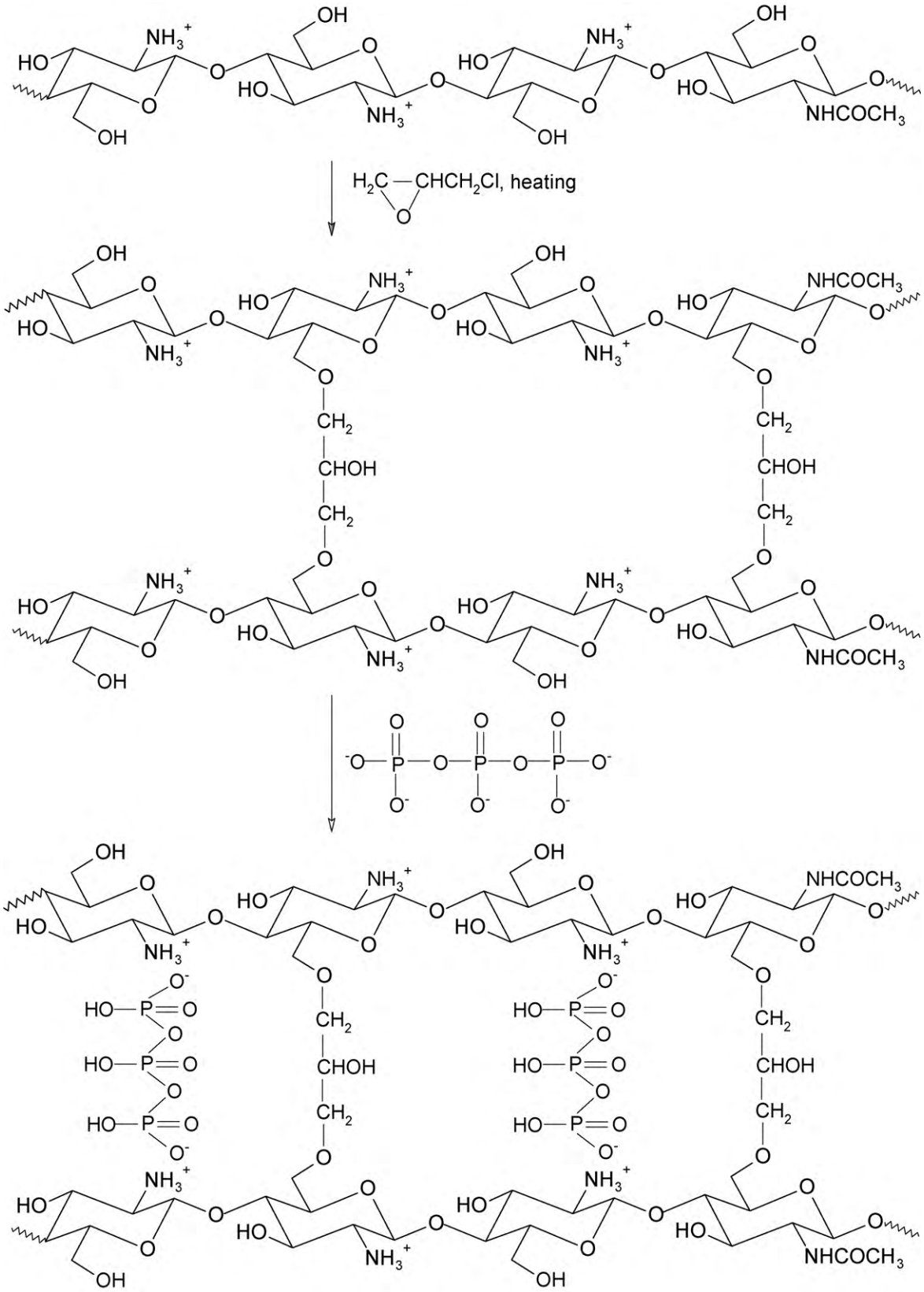

Fig. 1. Crosslinking of chitosan with epichlorohydrin and triphosphate.

the solutions were removed and then diluted in volumetric flasks. The remaining concentrations of Cu(II), Cd(II) and Pb(II) ions were determined by FAAS at wavelengths of 324.8, 228.8 and 283.3 nm, respectively.

2.5.2. Adsorption kinetics

The time required for the system to reach equilibrium conditions was established using 150.0 mg of CTS–ECH–TPP and 200.0 mL of solutions with fixed concentration: 100 mg L^{-1} for Cu(II) ions and

50 mg L^{-1} for Cd(II) and Pb(II) ions, buffered at optimum pH (determined in advance for each metal ion) and stirred for 72 h. After pre-established time periods, the stirring was halted and aliquots (200 μL) of the supernatant were removed and diluted to an adequate volume. The remaining concentrations of metal ions were then determined by FAAS.

2.5.3. Adsorption isotherms

Adsorption equilibrium experiments were carried out using 50.0 mg of CTS–ECH–TPP placed in closed flasks containing 50.0 mL of Cu(II), Cd(II) or Pb(II) ion solutions, in various concentrations (10–500 mg L^{-1}) and buffered at optimum pH. After the adsorption equilibrium was reached, aliquots were removed and diluted in order to determine the remaining concentrations of metal ions by FAAS.

2.5.4. Desorption studies

For the desorption studies, 20.0 mg of CTS–ECH–TPP were added to 50.0 mL of 25 mg L^{-1} Cu(II), Cd(II) or Pb(II) ion solutions, buffered at optimum pH and kept under stirring for 48 h. The M^{2+}–CTS–ECH–TPP complex was collected by filtration and washed several times with distilled water to remove any unabsorbed metal ions and oven dried at 60 °C. The amount of Cu(II), Cd(II) and Pb(II) ions adsorbed per gram of CTS–ECH–TPP was determined from the metal ion concentration remaining in each solution. The adsorbent samples containing each metal ion were placed in contact with 50.0 mL of H_2O, HNO_3, HCl, KCl, NH_4Cl and EDTA solutions, at different concentrations and maintained under stirring for 3 h. The amount of metal ions desorbed was then determined by FAAS.

The percentage of desorption was calculated from the following expression:

$$\text{desorption}(\%) = \frac{\text{amount of metal ions desorbed}}{\text{amount of metal ions adsorbed}} \times 100 \quad (8)$$

3. Results and discussion

3.1. Elemental (CHN) analysis and EDS

The C, H and N values for the CTS composition were 39.43%, 8.41% and 7.30%, respectively, and for the CTS–ECH–TPP adsorbent they were 29.00%, 7.44% and 4.78%, respectively. The semi-quantitative results obtained from the EDS revealed an atomic percentage of phosphorus in the new adsorbent of 4.46%. It was observed that there was a decrease in the percentage of C, H and N atoms and the presence of P atoms after the chitosan modification.

3.2. FTIR spectroscopy

The FTIR spectra for the CTS, TPP and CTS–ECH–TPP samples are shown in Fig. 2. The CTS–ECH–TPP spectrum (Fig. 2c) showed a new peak at 1554 cm^{-1}, which can be attributed to the ionic interaction between the positively charged amino groups of the crosslinked chitosan and the negatively charged groups of the triphosphate [5,22,23]. In addition, peaks at 1647, 1385 and 1081 cm^{-1} representing C=O stretching, C–H deformation and C–O stretching [24], respectively, were present in the chitosan spectrum (Fig. 2a) and peaks at 1225, 891 and 516 cm^{-1}, corresponding P=O stretching and deformation, were present in the TPP spectrum (Fig. 2b).

3.3. Thermalgravimetric analysis

The TGA and DSC thermograms for the CTS, TPP and CTS–ECH–TPP samples are shown in Fig. 3. The thermogravimetric profiles in Fig. 3a reveal two stages of mass loss. The first degradation stage at around 64–110 °C, with a mass loss of 2–10%, is related mainly to the loss of water physically adsorbed on the surface of the materials. In the second degradation stage, other mass losses are observed. The CTS undergoes a mass loss of 49.68% at 332.2 °C. The TPP shows mass losses of 2.66% and 0.87% at 140.8 and 255.6 °C, respectively. The second degradation stage of CTS–ECH–TPP was observed at 231.6 °C with a mass loss of 37.75%. The temperature of the second degradation stage of CTS–ECH–TPP is lower than that of the unmodified chitosan, which indicates that the new adsorbent is less thermally stable than chitosan.

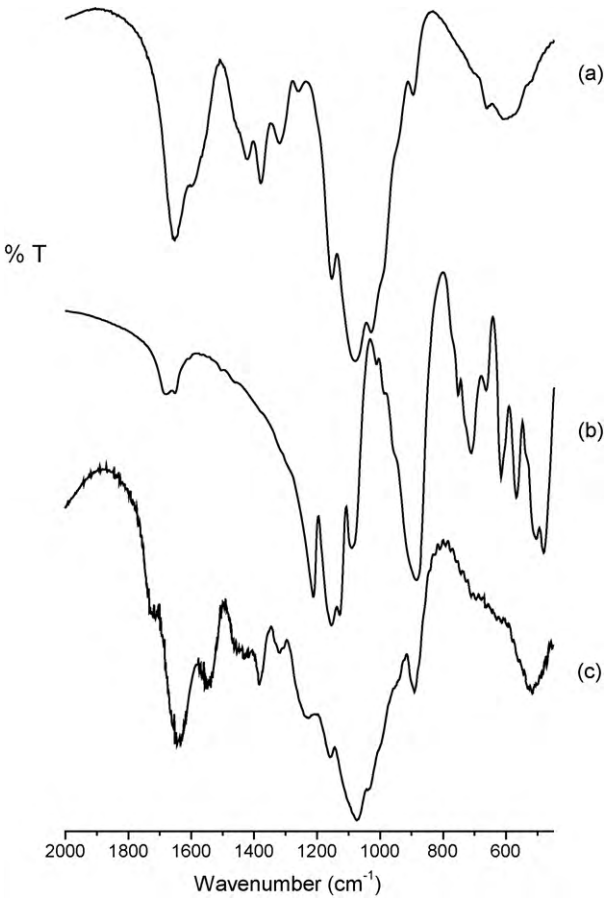

Fig. 2. Infrared spectra of: (a) CTS, (b) TPP and (c) CTS–ECH–TPP, using KBr pellets in the range of 2000–450 cm^{-1}.

In the DSC thermograms (Fig. 3b), an endothermic peak at around 88–120 °C, corresponding to water removal, can be observed for all samples. This is consistent with the results obtained by TGA. The DSC thermogram for CTS shows an exothermic peak at 308.6 °C, while that for TPP shows a small exothermic peak at 207.1 °C. In the DSC thermogram for CTS–ECH–TPP three exothermic peaks can be observed, at 209.1, 235.4 and 282.6 °C. These exothermic peaks can be attributed to the thermal degradation of the materials. A significant difference in the position of the exothermic peaks of CTS and CTS–ECH–TPP was observed, which indicates surface modification of the chitosan.

The characterization results confirmed that the formation of the new adsorbent (CTS–ECH–TPP) occurred successfully.

3.4. Potentiometric equilibrium determination

The potentiometric equilibrium curve of the adsorbent (Fig. 4a) shows three points of inflection, which corresponds to the neutralization of three protons of the CTS–ECH–TPP.

The formation constant of the H_3CTS–ECH–TPP (Eq. (9)) as well as the acid dissociation constants (pK_a), defined by Eqs. (10)–(12),

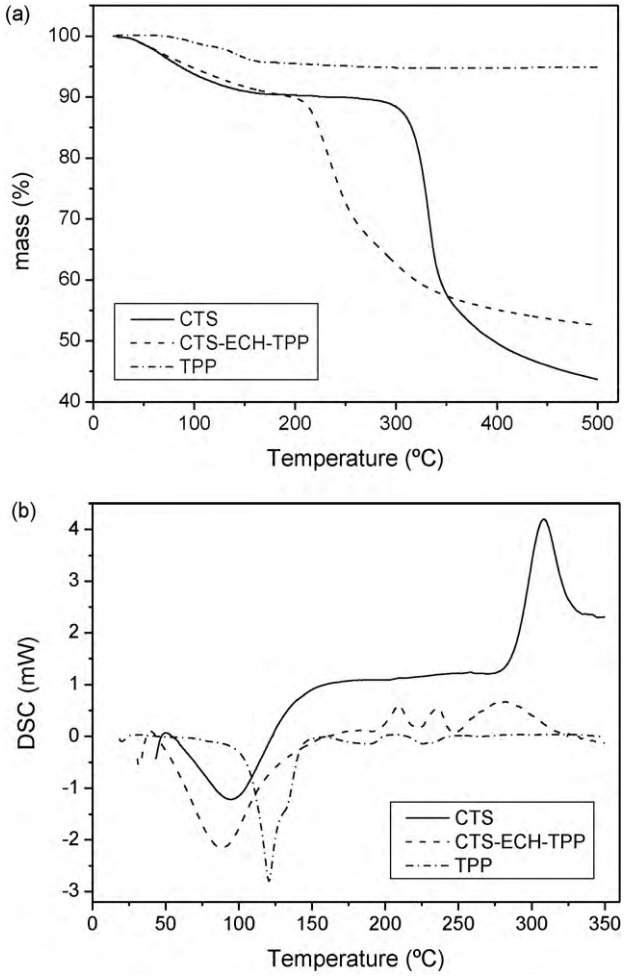

Fig. 3. TGA (a) and DSC (b) thermograms of CTS, TPP and CTS–ECH–TPP. The samples were analyzed under nitrogen flow at a rate of 50 mL min^{-1} and at a heating rate of 10 °C min^{-1}.

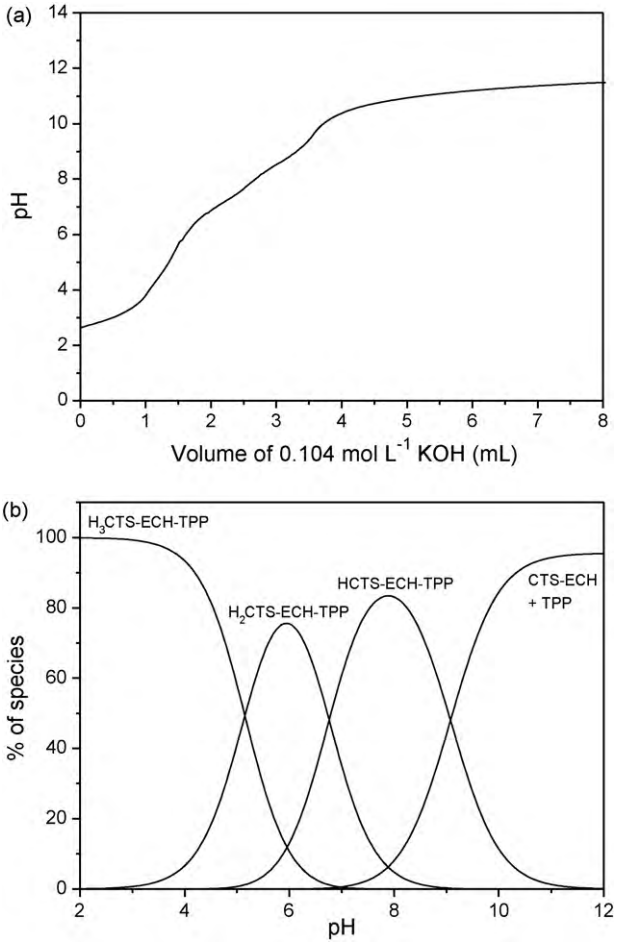

Fig. 4. (a) Curve of potentiometric equilibrium and (b) species distribution curves for H_3CTS–ECH–TPP as a function of pH.

were calculated from the potentiometric data.

$$\text{TPP} + \text{CTS–ECH} \rightleftharpoons \text{H}_3\text{CTS–ECH–TPP} \quad (\log K = 10.71) \tag{9}$$

$$\text{H}_3\text{CTS–ECH–TPP} + \text{OH}^- \rightleftharpoons \text{H}_2\text{CTS–ECH–TPP} + \text{H}_2\text{O} \quad (\text{p}K_{a1} = 5.14) \tag{10}$$

$$\text{H}_2\text{CTS–ECH–TPP} + \text{OH}^- \rightleftharpoons \text{HCTS–ECH–TPP} + \text{H}_2\text{O} \quad (\text{p}K_{a2} = 6.76) \tag{11}$$

$$\text{HCTS–ECH–TPP} + \text{OH}^- \rightleftharpoons \text{TPP} + \text{CTS–ECH} + \text{H}_2\text{O} \quad (\text{p}K_{a3} = 9.08) \tag{12}$$

The species distribution curves for H_3CTS–ECH–TPP as a function of pH are shown in Fig. 4b. It can be observed that the tri-protonated adsorbent (H_3CTS–ECH–TPP) predominates at pH values below 4.5, and its deprotonation leads to the formation of the di-protonated form (H_2CTS–ECH–TPP), which has a maximum formation at pH 5.9. This species undergoes deprotonation resulting in the mono-protonated form (HCTS–ECH–TPP), which has a maximum formation of 83% at pH 8.0 and decreases with increasing pH, giving rise to the free and completely deprotonated TPP. The TPP appears in the solution at above pH 7.0, when the disruption of electrostatic interactions and hydrogen bonds between the TPP and CTS–ECH begins.

3.5. Effect of pH

The pH of the aqueous solution is an important parameter in adsorption processes. In this study, the effect of pH on the adsorption of Cu(II) and Cd(II) ions onto CTS–ECH–TPP was studied in the pH range of 2–11, while for the adsorption of Pb(II) ions the study was performed at pH 2–5, since the precipitation of lead(II) hydroxide was observed at higher pH. The buffer solutions were used to adjust the pH and as auxiliary complexing agents to prevent the precipitation of Cu(II) and Cd(II) ions.

Fig. 5 shows the effect of pH on the adsorption of Cu(II), Cd(II) and Pb(II) ions by CTS–ECH–TPP. It was observed that the amount of Cu(II) ions adsorbed increases with solution pH up to almost pH 6.0 and then decreases with increasing pH. A similar pattern was observed for Cd(II) ions, but the maximum amount adsorbed was reached at pH 7.0. However, the optimum pH for the adsorption of Pb(II) ions was 5.0.

At acid pH, the adsorbent surface will be completely covered with hydronium ions which compete strongly with metal ions for adsorption sites. With an increase in pH, the concentration of H_3O^+ ions decreases, facilitating the adsorption of metal ions by the adsorbent [25]. At alkaline pH, it was observed that the adsorption of Cu(II) and Cd(II) ions by CTS–ECH–TPP decreased significantly, since the results of the potentiometric titration (Fig. 4)

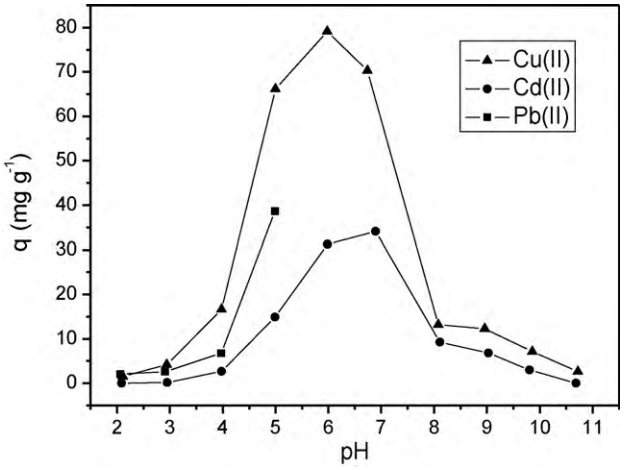

Fig. 5. Effect of pH on adsorption of Cu(II), Cd(II) and Pb(II) ions by CTS–ECH–TPP. Volume = 50.0 mL; [Cu^{2+}, Cd^{2+} or Pb^{2+}] = 50 mg L^{-1}; adsorbent mass = 50.0 mg; temperature = 25 °C; stirring = 200 rpm.

showed that at pH values above 7.0 there are no longer ionic interactions between the phosphate groups of the triphosphate and the amino groups of the chitosan. The triphosphate complexed with the metal ions then moves to the solution and the adsorption capacity decreases, reaching values close to zero at around pH 11, where the interaction between the chitosan and triphosphate ceases.

3.6. Adsorption kinetics

The adsorption kinetics for Cu(II), Cd(II) and Pb(II) ion adsorption by CTS–ECH–TPP is represented in Fig. 6. The kinetic curves show that the adsorption equilibrium was reached in approximately 30 h for Cu(II) ions, 10 h for Cd(II) and 12 h for Pb(II), and then remained constant until the end of the experiment (72 h).

In order to determine the kinetic mechanism for the adsorption of metal ions by CTS–ECH–TPP, the non-linear and linear forms of pseudo-first-order (PFO) and pseudo-second-order (PSO) models were used to interpret the experimental data, according to Eqs. (13), (14), (15) and (16), respectively [2,7,12,26]:

$$q_t = q_e[1 - \exp(-k_1 t)] \tag{13}$$

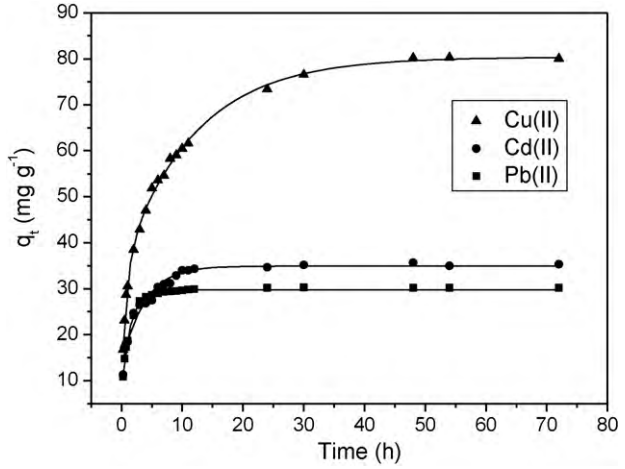

Fig. 6. Adsorption kinetics of Cu(II), Cd(II) and Pb(II) ion adsorption by CTS–ECH–TPP. Volume = 200.0 mL; [Cu^{2+}] = 100 mg L^{-1} and [Cd^{2+} or Pb^{2+}] = 50 mg L^{-1}; pH 6.0 for Cu(II), 7.0 for Cd(II) and 5.0 for Pb(II); adsorbent mass = 150.0 mg; temperature = 25 °C; stirring = 200 rpm.

Table 1
Kinetic models evaluated for adsorption of Cu(II), Cd(II) and Pb(II) ions by CTS–ECH–TPP.

Metal ions	Cu(II)	Cd(II)	Pb(II)
Non-linear PFO			
$q_{e,calc}$ (mg g^{-1})	72.50	32.52	29.42
k_1 (h^{-1})	0.279	0.954	1.179
R^2	0.818	0.829	0.957
%D	19.19	10.76	4.52
Linear PFO			
$q_{e,calc}$ (mg g^{-1})	50.87	20.44	15.35
k_1 (h^{-1})	0.118	0.281	0.452
R^2	0.986	0.958	0.979
%D	55.18	52.34	56.33
Non-linear PSO			
$q_{e,calc}$ (mg g^{-1})	78.44	35.09	31.12
k_2 (g mg^{-1} h^{-1})	5.84×10^{-3}	3.78×10^{-2}	5.91×10^{-2}
R^2	0.934	0.952	0.989
%D	11.88	5.67	1.97
Linear PSO			
$q_{e,calc}$ (mg g^{-1})	83.61	35.87	30.42
k_2 (g mg^{-1} h^{-1})	4.18×10^{-3}	3.16×10^{-2}	9.25×10^{-2}
R^2	0.998	0.999	0.999
%D	9.98	5.67	1.93

$$\log(q_e - q_t) = \log q_e - \frac{k_1}{2.303} t \tag{14}$$

$$q_t = \frac{k_2 q_e^2 t}{1 + k_2 q_e t} \tag{15}$$

$$\frac{t}{q_t} = \frac{1}{k_2 q_e^2} + \frac{1}{q_e} t \tag{16}$$

where q_e and q_t are the amount adsorbed (mg g^{-1}) at equilibrium and at time t (h), respectively, k_1 is the rate constant of PFO adsorption (h^{-1}) and k_2 is the rate constant of PSO adsorption (g mg^{-1} h^{-1}).

The most appropriate model through which to evaluate the kinetic mechanism of adsorption was selected based on the highest values for the average absolute percentage deviation (%D) and correlation coefficient (R^2) obtained.

The %D values were calculated as follows:

$$\%D = \left(\frac{1}{N} \sum_{i=1}^{N} \left| \frac{q_{e,exp} - q_{e,calc}}{q_{e,exp}} \right| \right) \times 100 \tag{17}$$

The results for the kinetic parameters for the adsorption of Cu(II), Cd(II) and Pb(II) ions are given in Table 1.

It can be observed that the PFO model (in the non-linear and linear forms) gave %D values higher than those obtained with the PSO model. In addition, the calculated amounts adsorbed ($q_{e,calc}$) were significantly different from the experimental amounts adsorbed ($q_{e,exp}$), which were 80.19 mg g^{-1} for Cu(II), 34.33 mg g^{-1} for Cd(II) and 29.88 mg g^{-1} for Pb(II). Therefore, the results indicate that the PFO model is not appropriate for the determination of the kinetic mechanism of adsorption of Cu(II), Cd(II) and Pb(II) ions onto CTS–ECH–TPP.

The experimental data for the adsorption kinetics of Cu(II), Cd(II) and Pb(II) ion adsorption onto CTS–ECH–TPP were better fitted with the use of a linear PSO model, which provided the best %D and R^2 values. Moreover, there was a small difference between $q_{e,calc}$ and $q_{e,exp}$, with relative errors of 4.3% for Cu(II), 4.5% for Cd(II) and 1.8% for Pb(II).

Several studies in the literature involving adsorption of Cu(II), Cd(II) and Pb(II) ions, as well as other metal ions, onto chitosan or modified chitosan, have also shown that the PSO kinetics model gave the best fit for the experimental data [2,3,7,8,12,24,26–31].

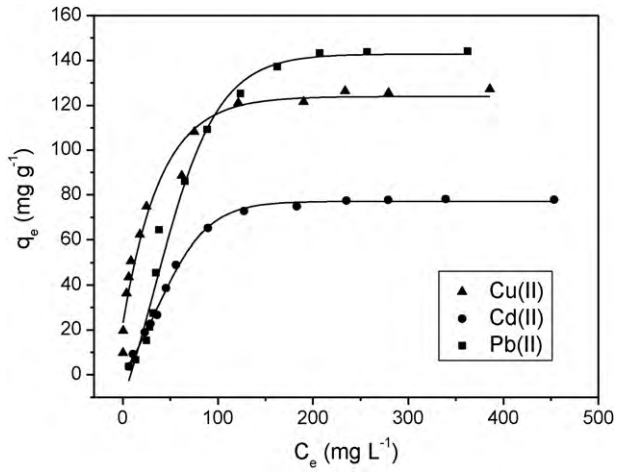

Fig. 7. Adsorption equilibrium isotherm of Cu(II), Cd(II) and Pb(II) ion adsorption by CTS–ECH–TPP. Volume = 50.0 mL; [Cu^{2+}, Cd^{2+} or Pb^{2+}] = 10–500 mg L^{-1}; pH 6.0 for Cu(II), 7.0 for Cd(II) and 5.0 for Pb(II); adsorbent mass = 50.0 mg; temperature = 25 °C; stirring = 200 rpm.

3.7. Adsorption isotherms

Fig. 7 shows the adsorption equilibrium isotherm obtained for Cu(II), Cd(II) and Pb(II) ion adsorption onto CTS–ECH–TPP. In this figure the relationship between the amount of metal ion adsorbed onto the adsorbent surface and the remaining metal ion concentration in the aqueous phase at equilibrium can be observed. This relationship showed that the adsorption capacity increased with the equilibrium concentration of the metal ion in solution, progressively reaching saturation of the adsorbent.

3.7.1. Langmuir isotherm

The experimental adsorption data were fitted according to the Langmuir isotherm model, this equation (Eq. (18)) being preferentially used in studies on adsorption in solution, where q_e and C_e are the amount adsorbed (mg g^{-1}) and the adsorbate concentration in solution (mg L^{-1}), respectively, both at equilibrium. K_L is the Langmuir constant (L mg^{-1}) and q_m is the maximum adsorption capacity of the monolayer formed on the adsorbent (mg g^{-1}) [26].

$$q_e = \frac{K_L C_e q_m}{1 + K_L C_e} \tag{18}$$

The Langmuir model assumes that the adsorbent surface has sites of identical energy and that each adsorbate molecule is located at a single site; hence, it predicts the formation of a monolayer of the adsorbate on the adsorbent surface [3].

The linear form of the Langmuir isotherm, represented by Eq. (19), is employed to determine the q_m and K_L values from the angular and linear coefficients obtained by plotting C_e/q_e as a function of C_e, which are given in Table 2.

$$\frac{C_e}{q_e} = \frac{1}{K_L q_m} + \frac{C_e}{q_m} \tag{19}$$

3.7.2. Freundlich isotherm

The Freundlich isotherm is one of the most widely used isotherms for the description of adsorption equilibrium. This isotherm is an empirical equation employed to describe equilibrium on heterogeneous surfaces and hence does not assume monolayer capacity. Mathematically, it is expressed by

$$q_e = K_F C_e^{1/n} \tag{20}$$

Table 2
Adsorption isotherm parameters for adsorption of Cu(II), Cd(II) and Pb(II) ions by CTS–ECH–TPP.

Metal ions	Cu(II)	Cd(II)	Pb(II)
Non-linear Langmuir			
q_m (mg g^{-1})	130.38	98.16	215.74
K_L (L mg^{-1})	6.38×10^{-2}	1.46×10^{-2}	8.48×10^{-3}
R^2	0.965	0.957	0.932
%D	13.44	14.69	16.10
Linear Langmuir			
q_m (mg g^{-1})	130.72	83.75	166.94
K_L (L mg^{-1})	8.44×10^{-2}	3.91×10^{-2}	2.20×10^{-2}
R^2	0.998	0.997	0.990
%D	13.10	15.29	12.18
Non-linear Freundlich			
K_F (mg g^{-1})	29.74	8.04	7.29
n	3.80	2.49	1.85
R^2	0.958	0.854	0.855
%D	16.25	27.46	21.62
Linear Freundlich			
K_F (mg g^{-1})	20.76	1.21	11.32
n	2.64	1.14	2.04
R^2	0.986	0.978	0.970
%D	16.16	33.70	25.02
Non-linear D-R			
q_m (mg g^{-1})	120.34	81.70	155.51
k (mol^2 kJ^{-2})	-4.71×10^{-3}	-1.97×10^{-3}	-2.60×10^{-3}
R^2	0.935	0.989	0.985
%D	24.05	19.57	21.25
Linear D-R			
q_m (mg g^{-1})	124.72	2.18	385.54
k (mol^2 kJ^{-2})	-5.92×10^{-3}	-6.06×10^{-3}	-3.53×10^{-3}
R^2	0.985	0.964	0.970
%D	28.58	77.57	81.70

Eq. (20) can also be expressed in the linearized logarithmic form as

$$\log q_e = \log K_F + \frac{1}{n} \log C_e \tag{21}$$

where K_F and n are the Freundlich isotherm constants indicating the adsorption capacity (mg g^{-1}) and adsorption intensity (unitless), respectively [12,32]. The results calculated for the Freundlich isotherm constants are given in Table 2.

3.7.3. Dubinin-Radushkevich isotherm

Although the Langmuir and Freundlich isotherm models are widely used, they do not give information on the adsorption mechanism. To this aim, the equilibrium data were tested with the Dubinin-Radushkevich isotherm model (D-R isotherm). This isotherm model predicts the nature of the adsorbate sorption onto the adsorbent and it is used to calculate the mean free energy of sorption. The non-linear D-R isotherm is expressed as:

$$q_e = q_m \exp(-k\varepsilon^2) \tag{22}$$

and the linearized form of the equation is given as:

$$\ln q_e = \ln q_m - k\varepsilon^2 \tag{23}$$

where q_e is the amount of solute adsorbed per mass of adsorbent (g g^{-1}), q_m is the maximum adsorption capacity (g g^{-1}), k is the D-R constant (mol^2 kJ^{-2}) and ε is the Polanyi potential (J mol^{-1}), which can be calculated as:

$$\varepsilon = RT \ln\left(1 + \frac{1}{C_e}\right) \tag{24}$$

where R is the gas constant (J mol^{-1} K^{-1}), T the absolute temperature (K) and C_e the equilibrium concentration of the adsorbate in aqueous solution (g L^{-1}) [1,33].

The values of q_m and k were calculated and are shown in Table 2.

Table 3
Maximum adsorption capacity of various chitosan samples modified for adsorption of Cu(II), Cd(II) and Pb(II) ions reported in the literature.

Adsorbent	q_m (mg g^{-1})			Reference
	Cu(II)	Cd(II)	Pb(II)	
Chitosan	45.2	–	–	[34]
Chitosan microspheres	80.71	–	–	[35]
Chitosan	–	105	–	[36]
Chitosan	–	–	115.6	[37]
Chitosan	37.88	–	13.05	[1]
Chitosan crosslinked with EGDE	45.94	–	–	[35]
Chitosan crosslinked with GLA	59.67	–	–	[35]
Chitosan crosslinked with ECH	62.47	–	–	[35]
Chitosan microspheres crosslinked with ECH	39.31	–	–	[24]
Chitosan modified with Reactive Blue 2 dye	57.0	–	–	[2]
Chitosan modified with H_2fmbme complexing agent	113.6	–	–	[3]
chitosan–tripolyphosphate chelating resin	200	–	–	[5]
Chitosan functionalized with xanthate	–	–	322.6	[31]
chitosan–pectin pellets	–	1.23	11.2	[38]
Procion Green H-4G immobilized pHEMA/chitosan	–	43.60	68.81	[39]
Chitosan crosslinked with ECH	35.46	–	34.13	[1]
GLA-crosslinked metal-complexed chitosans	33.00	–	105.26	[30]
Chitosan modified with sulphoxine chelant agent	53.8	32.9	–	[28,29]
Chitosan modified with Reactive Orange 16 dye	107.3	90.3	–	[27]
Chitosan modified with BPMAMF complexing agent	109	38.5	–	[26]
Chitosan crosslinked with ECH–TPP	130.72	83.75	166.94	Present study

On analyzing the values of %*D* and R^2 obtained using three isotherm models, it can be observed that the Langmuir equation in the linear form provided the best fit for the experimental data. Thus, this isotherm model was used to interpret the adsorption of metal ions by the CTS–ECH–TPP adsorbent.

The maximum adsorption capacities (q_m) for Cu(II), Cd(II) and Pb(II) ion adsorption onto other modified chitosan adsorbents, preparation under different conditions, reported in the literature, are compared in Table 3. It can be seen that the q_m value varies considerably for different adsorbents and that, by comparison, the CTS–ECH–TPP system exhibits a good capacity to adsorb Cu(II), Cd(II) and Pb(II) ions from aqueous solutions.

The mean free energy of adsorption (E) was calculated from the k values using the equation:

$$E = \frac{1}{\sqrt{-2k}} \quad (25)$$

The E value is used to ascertain the type of adsorption process under consideration. If this value is between 8 and 16 kJ mol^{-1}, the adsorption process can be assumed to involve chemical sorption. On the other hand, values lower than 8 kJ mol^{-1} indicate that the adsorption process is of a physical nature [40,41].

In this study, the E values obtained using the D-R constant, in the non-linear form, were 10.3 kJ mol^{-1} for Cu(II), 15.9 kJ mol^{-1} for Cd(II) and 13.9 kJ mol^{-1} for Pb(II), indicating that the adsorption of these ions onto CTS–ECH–TPP occurs via a chemical process.

3.8. Desorption of Cu(II), Cd(II) and Pb(II) ions

Desorption studies are important to investigate the possibility for the recovery of metals adsorbed on the adsorbent surface, as well as for the regeneration of the adsorbent for subsequent reuse.

In this study, H_2O, HNO_3, HCl, KCl, NH_4Cl and EDTA solutions, at different concentrations, were used as eluents. The percentages of Cu(II), Cd(II) and Pb(II) ion desorption for each eluent are listed in Table 4. It was observed that highest desorption values for Cu(II) and Cd(II) ions (88.7% and 89.9%, respectively) were obtained using a 1 mol L^{-1} HNO_3 solution. The 0.1 mol L^{-1} HNO_3, HCl and EDTA solutions also showed good desorption results (around 88%). However, KCl and NH_4Cl were not efficient eluents in the desorption of Cu(II) and Cd(II) ions adsorbed on the adsorbent surface. For the desorption of Pb(II) ions, the best performance was obtained with HCl solutions, values being slightly higher at a concentration of 1 mol L^{-1} (79.2%). The HNO_3 solutions also showed good performance for the desorption of Pb(II) ions, obtaining values close to those achieved using HCl solutions.

Ngah et al. [35] using EDTA in various concentrations (10^{-2} to 10^{-6} mol L^{-1}) for the desorption of Cu(II) ions from chitosan and chitosan microspheres crosslinked with GLA, ECH and EGDE, obtained desorption values of 97.7%, 95.4% and 82.3% for Cu(II) ions adsorbed on chitosan–ECH, chitosan–GLA and chitosan–EGDE, respectively, using 10^{-2} mol L^{-1} EDTA, and 65.2% for Cu(II) ions adsorbed on chitosan using 10^{-4} mol L^{-1} EDTA.

Vasconcelos et al. [2], using EDTA in concentrations of 0.1, 0.01 and 0.001 mol L^{-1} for desorption of Cu(II) ions from chitosan microspheres modified with Reactive Blue 2 dye, obtained desorption values of 80.3%, 88.7% and 89.8%, respectively.

Chauhan and Sankararamakrishnan [31] studied the desorption of Pb(II) ions adsorbed on chitosan functionalized with xanthate using the following eluents, 0.01 mol L^{-1} EDTA, 0.01 mol L^{-1} HCl and 0.5 mol L^{-1} NaOH. The results showed only 26% desorption when NaOH was used and 48% when EDTA and HCl were used.

Chen et al. [30] used EDTA in concentrations of 1.00, 0.50 and 0.25 mmol L^{-1} for desorption of Cu(II), Zn(II), Ni(II) and Pb(II) ions

Table 4
Percentages of Cu(II), Cd(II) and Pb(II) ion desorption from M^{2+}–CTS–ECH–TPP complex.

Eluent	Concentration (mol L^{-1})	Desorption (%)		
		Cu(II)	Cd(II)	Pb(II)
H_2O	–	0.62	0.84	0.75
HNO_3	0.1	87.9	88.5	76.4
HNO_3	1	88.7	89.9	76.9
HNO_3	3	87.0	87.2	76.1
HCl	0.1	87.2	87.8	78.2
HCl	1	88.2	89.0	79.2
HCl	3	86.7	87.0	77.7
KCl	1	2.9	33.0	61.0
KCl	3	4.6	46.3	63.2
NH_4Cl	1	11.2	46.6	30.1
NH_4Cl	3	34.4	47.7	54.3
EDTA	0.1	87.6	88.2	55.1
EDTA	0.01	84.9	88.0	53.5
EDTA	0.001	64.0	86.5	52.5

adsorbed on glutaraldehyde-crosslinked metal-complexed chitosan samples. The best results were obtained using 1.00 mmol L^{-1} EDTA, reaching desorption values of around 70% for Cu(II), 50% for Pb(II) and 30% for Zn(II) and Ni(II).

4. Conclusions

The modification of chitosan was confirmed by CHN analysis, EDS, FTIR spectroscopy, TGA and DSC.

The adsorption of Cu(II), Cd(II) and Pb(II) ions was shown to be dependent on the solution pH, and the optimum pH values for the adsorption were 6.0, 7.0 and 5.0, respectively.

The kinetics study demonstrated that the kinetic mechanism for the adsorption of metal ions followed a pseudo-second-order model, which provided the best experimental data correlation.

The Langmuir isotherm model provided the best fit for the experimental adsorption data for these ions, revealing maximum adsorption capacities for Cu(II), Cd(II) and Pb(II) ions of 130.72, 83.75 and 166.94 mg g^{-1}, respectively.

From the Dubinin-Radushkevich isotherm, the values of the mean free energy of adsorption revealed that the adsorption mechanism is predominantly due to a chemical process.

The desorption of Cu(II), Cd(II) and Pb(II) ions demonstrated that the best desorption performance was obtained with HNO_3 and HCl as eluents.

The results suggested that the new adsorbent could be used in processes of separation, preconcentration and Cu(II), Cd(II) or Pb(II) ion uptake from aqueous solutions.

Acknowledgements

The authors wish to thank Conselho Nacional de Pesquisa e Desenvolvimento–CNPq, Brazil for financial support.

References

[1] A.H. Chen, S.C. Liu, C.Y. Chen, C.Y. Chen, Comparative adsorption of Cu(II), Zn(II), and Pb(II) ions in aqueous solution on the crosslinked chitosan with epichlorohydrin, J. Hazard. Mater. 154 (2008) 184–191.
[2] H.L. Vasconcelos, V.T. Fávere, N.S. Gonçalves, M.C.M. Laranjeira, Chitosan modified with Reactive Blue 2 dye on adsorption equilibrium of Cu(II) and Ni(II) ions, React. Funct. Polym. 67 (2007) 1052–1060.
[3] H.L. Vasconcelos, T.P. Camargo, N.S. Gonçalves, A. Neves, M.C.M. Laranjeira, V.T. Fávere, Chitosan crosslinked with a metal complexing agent: synthesis, characterization and copper(II) ions adsorption, React. Funct. Polym. 68 (2008) 572–579.
[4] M.S. Chiou, H.Y. Li, Adsorption behavior of reactive dye in aqueous solution on chemical cross-linked chitosan beads, Chemosphere 50 (2003) 1095–1105.
[5] S.T. Lee, F.L. Mi, Y.J. Shen, S.S. Shyu, Equilibrium and kinetic studies of copper(II) ion uptake by chitosan–tripolyphosphate chelating resin, Polymer 42 (2001) 1879–1892.
[6] J. Fangkangwanwong, R. Yoksan, S. Chirachanchai, Chitosan gel formation via the chitosan–epichlorohydrin adduct and its subsequent mineralization with hydroxyapatite, Polymer 47 (2006) 6438–6445.
[7] F.C. Wu, R.L. Tseng, R.S. Juang, Kinetic modeling of liquid-phase adsorption of reactive dyes and metal ions on chitosan, Water Res. 35 (2001) 613–618.
[8] L. Zhou, Y. Wang, Z. Liu, Q. Huang, Characteristics of equilibrium, kinetics studies for adsorption of Hg(II), Cu(II), and Ni(II) ions by thiourea-modified magnetic chitosan microspheres, J. Hazard. Mater. 161 (2009) 995–1002.
[9] M. Rinaudo, Chitin and chitosan: properties and applications, Prog. Polym. Sci. 31 (2006) 603–632.
[10] A.J. Varma, S.V. Deshpande, J.F. Kennedy, Metal complexation by chitosan and its derivatives: a review, Carbohydr. Polym. 55 (2004) 77–93.
[11] T. Becker, M. Schlaak, H. Strasdeit, Adsorption of nickel(II), zinc(II) and cadmium(II) by new chitosan derivatives, React. Funct. Polym. 44 (2000) 289–298.
[12] W.S.W. Ngah, A. Kamari, Y.J. Koay, Equilibrium and kinetics studies of adsorption of copper(II) on chitosan and chitosan/PVA beads, Int. J. Biol. Macromol. 34 (2004) 155–161.
[13] A.O. Martins, E.L. Silva, E. Carasek, N.S. Gonçalves, M.C.M. Laranjeira, V.T. Fávere, Chelating resin from functionalization of chitosan with complexing agent 8-hydroxyquinoline: application for metal ions on line preconcentration system, Anal. Chim. Acta 521 (2004) 157–162.
[14] M.M. Beppu, E.J. Arruda, R.S. Vieira, N.N. Santos, Adsorption of Cu(II) on porous chitosan membranes functionalized with histidine, J. Membr. Sci. 240 (2004) 227–235.
[15] E. Guibal, N.V.O. Sweeney, T. Vincent, J.M. Tobin, Sulfur derivatives of chitosan for palladium sorption, React. Funct. Polym. 50 (2002) 149–163.
[16] E. Guibal, Interactions of metal ions with chitosan–based sorbents: a review, Sep. Purif. Technol. 38 (2004) 43–74.
[17] V.L. Gonçalves, M.C.M. Laranjeira, V.T. Fávere, R.C. Pedrosa, Effect of crosslinking agents on chitosan microspheres in controlled release of diclofenac sodium, Polímeros 15 (2005) 6–12.
[18] A.K. Anal, W.F. Stevens, C.R. López, Ionotropic cross-linked chitosan microspheres for controlled release of ampicillin, Int. J. Pharm. 312 (2006) 166–173.
[19] J.A. Ko, H.J. Park, S.J. Hwang, J.B. Park, J.S. Lee, Preparation and characterization of chitosan microparticles intended for controlled drug delivery, Int. J. Pharm. 249 (2002) 165–174.
[20] P. Rasković, Step-by-step process integration method for the improvements and optimization of sodium tripolyphosphate process plant, Energy 32 (2007) 983–998.
[21] A.E. Martell, R.J. Motekaitis, Determination and Use of Stability Constants, second ed., VCH Publishers, New York, 1992.
[22] R. Laus, M.C.M. Laranjeira, A.O. Martins, V.T. Fávere, R.C. Pedrosa, J.C. Benassi, R. Geremias, Chitosan microspheres crosslinked with tripolyphosphate used for the removal of the acidity, iron (III) and manganese (II) in water contaminated in coal mining, Quim. Nova 29 (2006) 34–39.
[23] M.R. Moura, F.A. Aouada, R.J. Avena-Bustillos, T.H. McHugh, J.M. Krochta, L.H.C. Mattoso, Improved barrier and mechanical properties of novel hydroxypropyl methylcellulose edible films with chitosan/tripolyphosphate nanoparticles, J. Food Eng. 92 (2009) 448–453.
[24] T.C. Coelho, R. Laus, A.S. Mangrich, V.T. Fávere, M.C.M. Laranjeira, Effect of heparin coating on epichlorohydrin cross-linked chitosan microspheres on the adsorption of copper(II) ions, React. Funct. Polym. 67 (2007) 468–475.
[25] S.S. Gupta, K.G. Bhattacharyya, Adsorption of Ni(II) on clays, J. Colloid Interface Sci. 295 (2006) 21–32.
[26] K.C. Justi, V.T. Fávere, M.C.M. Laranjeira, A. Neves, R.A. Peralta, Kinetics and equilibrium adsorption of Cu(II), Cd(II), and Ni(II) ions by chitosan functionalized with 2[-bis-(pyridylmethyl)aminomethyl]-4-methyl-6-formylphenol, J. Colloid Interface Sci. 291 (2005) 369–374.
[27] H.L. Vasconcelos, E. Guibal, R. Laus, L. Vitali, V.T. Fávere, Competitive adsorption of Cu(II) and Cd(II) ions on spray-dried chitosan loaded with Reactive Orange 16, Mater. Sci. Eng. C 29 (2009) 613–618.
[28] L. Vitali, M.C.M. Laranjeira, V.T. Fávere, N.S. Gonçalves, Microencapsulation of the chelating agent sulfoxine into microspheres of chitosan prepared by spray drying as a new adsorbent for metalic ions, Quim. Nova 31 (2008) 1400–1404.
[29] L. Vitali, M.C.M. Laranjeira, N.S. Gonçalves, V.T. Fávere, Spray-dried chitosan microspheres containing 8-hydroxyquinoline-5 sulphonic acid as a new adsorbent for Cd(II) and Zn(II) ions, Int. J. Biol. Macromol. 42 (2008) 152–157.
[30] A.H. Chen, C.Y. Yang, C.Y. Chen, C.Y. Chen, C.W. Chen, The chemically crosslinked metal-complexed chitosans for comparative adsorptions of Cu(II), Zn(II), Ni(II) and Pb(II) ions in aqueous medium, J. Hazard. Mater. 163 (2009) 1068–1075.
[31] D. Chauhan, N. Sankararamakrishnan, Highly enhanced adsorption for decontamination of lead ions from battery wastewaters using chitosan functionalized with xanthate, Bioresour. Technol. 99 (2008) 9021–9024.
[32] J. Febrianto, A.N. Kosasih, J. Sunarso, Y.H. Ju, N. Indraswati, S. Ismadji, Equilibrium and kinetic studies in adsorption of heavy metals using biosorbent: a summary of recent studies, J. Hazard. Mater. 162 (2009) 616–645.
[33] S.S. Tripathy, A.M. Raichur, Abatement of fluoride from water using manganese dioxide-coated activated alumina, J. Hazard. Mater. 153 (2008) 1043–1051.
[34] C. Huang, Y.C. Chung, M.R. Liou, Adsorption of Cu(II) and Ni(II) by pelletized biopolymer, J. Hazard. Mater. 45 (1996) 265–277.
[35] W.S.W. Ngah, C.S. Endud, R. Mayanar, Removal of copper(II) ions from aqueous solution onto chitosan and cross-linked chitosan beads, React. Funct. Polym. 50 (2002) 181–190.
[36] J.R. Evans, W.G. Davids, J.D. MacRae, A. Amirbahman, Kinetics of cadmium uptake by chitosan–based crab shells, Water Res. 36 (2002) 3219–3226.
[37] J.C.Y. Ng, W.H. Cheung, G. McKay, Equilibrium studies for the sorption of lead from effluents using chitosan, Chemosphere 52 (2003) 1021–1030.
[38] A.L. Debbaudt, M.L. Ferreira, M.E. Gschaider, Theoretical and experimental study of M^{2+} adsorption on biopolymers. III. Comparative kinetic pattern of Pb, Hg and Cd, Carbohydr. Polym. 56 (2004) 321–332.
[39] Ö. Genç, L. Soysal, G. Bayramoğlu, M.Y. Arica, S. Bektaş, Procion Green H-4G immobilized poly(hydroxyethylmethacrylate/chitosan) composite membranes for heavy metal removal, J. Hazard. Mater. B97 (2003) 111–125.
[40] A. Özcan, A.S. Özcan, S. Tunali, T. Akar, I. Kiran, Determination of the equilibrium, kinetic and thermodynamic parameters of adsorption of copper(II) ions onto seeds of *Capsicum annuum*, J. Hazard. Mater. 124 (2005) 200–208.
[41] N. Ünlü, M. Ersoz, Adsorption characteristics of heavy metal ions onto a low cost biopolymer sorbent from aqueous solutions, J. Hazard. Mater. B136 (2006) 272–280.